Published for SISSA by Springer

Received: January 21, 2015
Revised: March 6, 2015
Accepted: March 10, 2015
Published: March 30, 2015

Search for new physics via photon polarization of $b \to s\gamma$

Naoyuki Haba,[a] **Hiroyuki Ishida,**[a] **Tsuyoshi Nakaya,**[b] **Yasuhiro Shimizu**[c,d] **and Ryo Takahashi**[a]

[a] *Graduate School of Science and Engineering, Shimane University, Matsue, 690-8504, Japan*
[b] *Department of Physics, Kyoto University, Kyoto, 606-8502, Japan*
[c] *Department of Physics, Tohoku University, Sendai, 980-8578 Japan*
[d] *Academic Support Center, Kogakuin University, Hachioji, 192-0015 Japan*

E-mail: haba@riko.shimane-u.ac.jp, ishida@riko.shimane-u.ac.jp, t.nakaya@scphys.kyoto-u.ac.jp, shimizu@tuhep.phys.tohoku.ac.jp, r.takahashi@m.tohoku.ac.jp

Abstract: We suggest a discriminant analysis of new physics beyond the standard model through a detection of photon polarization in a radiative B meson decay. This analysis is investigated in SUSY SU(5) GUT with right-handed neutrino and left-right symmetric models. New physics search via CP asymmetry in the same process are also evaluated in each model for comparison. We show that new physics can be found via detecting the photon polarization in a parameter space of TeV energy scale.

Keywords: Rare Decays, Beyond Standard Model, B-Physics

ArXiv ePrint: 1501.00668

doi:10.1007/JHEP03(2015)160

JHEP03(2015)160

Contents

JHEP03(2015)160

1 Introduction

In this decade, we have never seen an exotic elementary particle except for the most likely to the standard model (SM) Higgs boson which was discovered at the LHC experiment. This fact might imply that a scale of new physics (NP) is higher than the energy scale that the LHC can reach. Thus, it is important to consider the possibility that such exotics are hard to be directly produced by collider experiments even though the next LHC will become 14 TeV.

On the other hand, indirect searches become powerful way to explore the existence of NP and related phenomena beyond the SM even if a new particle is impossible to be produced directly. One popular approach is flavor physics. For instance, flavor changing processes such as $\mu \to e\gamma$ and $b \to s\gamma$ retain much information about NP. Models of supersymmetric grand unified theory (SUSY GUT) predict relatively large branching ratios

of $\mathrm{Br}(\mu \to e\gamma) \sim \mathcal{O}(10^{-15}\text{-}10^{-13})$ for the NP scale (the right-handed selectron mass) of $M_{\rm NP} \simeq (100\text{-}300)\,\mathrm{GeV}$ in an SU(5) case and $\mathrm{Br}(\mu \to e\gamma) \sim \mathcal{O}(10^{-13}\text{-}10^{-11})$ in an SO(10) case [1, 2]. Then, ref. [3] suggested that the measurement of the angular distribution of e with respect to the spin direction of the muon in the $\mu \to e\gamma$ process might distinguish among several extensions of the SM if the signal could be detected. This implies that the precise determination of the chirality of the final e state in the $\mu \to e\gamma$ process might become a clue to obtain the evidence of NP. This situation is adopted to the $b \to s\gamma$ process, i.e. one would be able to discriminate among the SM and NP such as SUSY GUT models, the left-right symmetric standard model (LRSM), and the Pati-Salam models and so on, if one could precisely determine the chirality of the final s quark. The b quark can radiative decay into the s quark in the B meson and the chirality of the s quark is almost determined as left-handed in the SM. Accordingly, if we find more right-handed s quarks in the process than ones expected in the SM, we can expect that some kind of NP must cause this phenomena.

How about the measurement of the chirality of the s quark in the $b \to s\gamma$ process for the NP search? One may naively think that the determination of chirality of quarks except for the top quark is impossible (the top quark can decay before the hadronization). The $b \to s\gamma$ process occurs through the dipole type operators, $\bar{s}_L \sigma_{\mu\nu} b F^{\mu\nu}$ ($\bar{s}_R \sigma_{\mu\nu} b F^{\mu\nu}$) which induce left- (right-) handed photon. The information on the chirality of the s quark is imprinted on the photon polarization. In addition, there is no parity violation in QCD, the relation between the chirality of the s quark and the photon polarization is unchanged even if the hadronization is taken into account. Therefore, one can determine the chirality of s quark in the $b \to s\gamma$ process from the measurement of photon polarization [4, 5]. In refs. [6, 7], the authors mentioned that the higher order correction may induce the right-handed photon even though it is in the SM.

At e^+e^- colliders, such as Belle and BaBar, B_d mesons, which are spin 0 particles, are produced from the $\Upsilon(4S)$ resonance. The photon polarization of the $B_d \to X_s\gamma$ decay is determined from measurements of hadronic angular distributions due to the conservation of angular momentum. The LHCb collaboration actually reported the result of observation of photon polarization by measuring the angular distribution of produced mesons in the $B \to K\pi\pi\gamma$ process [8].[1] In addition to the $B \to K\pi\pi\gamma$ process, there is another possibility to determine the photon polarization by the $B \to K^* l^+ l^-$ process. Although there exists a box diagram in the process, the radiative decay diagram (penguin) becomes dominant (the box diagram is suppressed) in a low invariant mass region of dileptons [9, 10] (see also [11]). The chirality of the s quark in the K^* meson can be lead by the chirality of photon due to the conservation of the spin. Then, it is important to discuss the possibility of the detection of the photon chirality. In this work, we will consider the $b \to s\gamma$ process. In particular, a ratio of the Wilson coefficients of a dipole operator and a polarization parameter of photon will be firstly evaluated at a typical point in a model of SUSY SU(5) GUT with the right-handed neutrino (N_R) and LRSM in order to clarify whether one can find an evidence of NP or distinguish among the SM and NP, or not.

[1] This issue tells us that the theorists have to clarify the prediction of photon polarization in each model.

JHEP03(2015)160

In addition to the determination of the photon chirality, the CP asymmetry in the $b \to s\gamma$ process which are direct CP asymmetry, $A_{\rm CP}(b \to s\gamma)$ and time-dependent CP asymmetry, $S_{\rm CP}(B \to K_s\pi^0\gamma)$, is also a sensitive observable to NP [12]. Actually, the CP violating effects from NP can be enough larger than the SM expectation as $A_{\rm CP}(b \to s\gamma) \simeq -0.5\%$. However, this CP violation is constrained by the other experiment, e.g. the chromo electric dipole moment (CEDM) [13], and it can be negligibly smaller than the SM one when the CP violating phase depending on the $b \to s\gamma$ process is accidentally small. We will also evaluate the magnitude of $A_{\rm CP}(b \to s\gamma)$ in the SUSY SU(5) GUT with N_R and the LRSM although the magnitude strongly depends on CP violating phases in the models. Furthermore, $S_{\rm CP}(B \to K_s\pi^0\gamma)$ can also become larger than the SM expectation as $S_{\rm CP}(B \to K_s\pi^0\gamma) \simeq -0.3$. We will show this value is insensitive to the CP phase. Then, we will compare experimental detectability for the models of NP between the determination of photon polarization and the observation of both CP asymmetry in the $b \to s\gamma$ process.

We will suggest that one can discriminate NP beyond the SM by the detection of photon polarization in $b \to s\gamma$ process. We will point out that time-dependent CP asymmetry is the most stringent constraint in our sample model point at the moment. However, it will actually turn out that the LHCb with $2\,{\rm fb}^{-1}$ for the determination of photon polarization may check the existence of NP scale up to several TeV in both models.

2 Photon polarization

We investigate the photon polarization in the radiative rare decay, $b \to s\gamma$, process in a SUSY SU(5) GUT with N_R and the LRSM for the search of NP. The Wilson coefficients C_7 and C_7' of the dipole operator for the $b \to s\gamma$ process are important for the analyses of photon polarization. The effective Hamiltonian reads

$$\mathcal{H}_{\rm eff} \supset -\frac{4G_F}{\sqrt{2}} V_{tb}V_{ts}^*(C_7O_7 + C_7'O_7'), \tag{2.1}$$

with the magnetic operator,

$$O_7 = \frac{e}{16\pi^2} m_b(\bar{s}\sigma^{\mu\nu}P_R b)F_{\mu\nu}, \tag{2.2}$$

where G_F is the Fermi constant, m_b is the bottom quark mass, $\sigma^{\mu\nu} = \frac{i}{2}[\gamma^\mu, \gamma^\nu]$, and $P_{R,L} = \frac{1}{2}(1 \pm \gamma_5)$ (e.g., see [14]). O_7' is obtained by replacing $L \leftrightarrow R$ in O_7. Because left-handed s quark comes from O_7 and right-handed one comes from O_7', we might be able to determine the chirality of s quark by the difference of Wilson coefficients.

When one considers physics beyond the SM, there might be additional contributions to C_7 and C_7' from NP. In these cases, we can generically describe C_7 and C_7' as $C_7 = C_7^{\rm SM} + C_7^{\rm NP}$ and $C_7' = C_7'^{\rm SM} + C_7'^{\rm NP}$, respectively. The coefficients at the b quark mass scale μ_b are given by the leading logarithmic calculations with QCD corrections to the $b \to s\gamma$ process,

$$C_7(\mu_b) = \eta^{\frac{16}{23}} C_7(m_W) + \frac{8}{3}(\eta^{\frac{14}{23}} - \eta^{\frac{16}{23}})C_8(m_W) + \sum_{i=1}^{8} h_i \eta^{a_i}, \tag{2.3}$$

$$C_7'(\mu_b) = \eta^{\frac{16}{23}} C_7'(m_W) + \frac{8}{3}(\eta^{\frac{14}{23}} - \eta^{\frac{16}{23}})C_8'(m_W), \tag{2.4}$$

JHEP03(2015)160

at the leading order where $\eta = \alpha_s(m_W)/\alpha_s(\mu_b)$, $\alpha_s \equiv g_s^2/(4\pi)$, g_s is the strong coupling constant, m_W is the W boson mass, and h_i and a_i are numerical coefficients [15–17]. C_8 is the coefficient of chromomagnetic operator

$$O_8 = \frac{g_s}{16\pi^2} m_b (\bar{s}\sigma^{\mu\nu} T^A P_R b) G^A_{\mu\nu}, \tag{2.5}$$

in the $\Delta F = 1$ effective Hamiltonian,

$$\mathcal{H}_{\rm eff} \supset -\frac{4G_F}{\sqrt{2}} V_{tb} V_{ts}^* (C_8 O_8 + C_8' O_8'), \tag{2.6}$$

where T^A are the generators of $\mathrm{SU}(3)_C$ and O_8' is also obtained by replacing $L \leftrightarrow R$ in O_8. And, we also describe $C_8 = C_8^{\rm SM} + C_8^{\rm NP}$ and $C_8' = C_8'^{\rm SM} + C_8'^{\rm NP}$ including contributions from NP.

2.1 Case of SUSY SU(5) with the right-handed neutrinos

2.1.1 Model

At first, we give a brief review of a model of SUSY SU(5) GUT with N_R. In a simple SU(5) GUT model, the final s quark must have the same chirality as in the SM. When there is N_R, a neutrino Yukawa coupling induces additional flavor mixings in the right-handed down squark which derives the opposite chirality of s quark. Thus, we adopt the model of SUSY SU(5) GUT with N_R. The superpotential in this model is given by

$$W = \frac{1}{4} f^u_{ij} \Psi_i \Psi_j H + \sqrt{2} f^d_{ij} \Psi_i \Phi_j \bar{H} + f^\nu_{ij} \Phi_i \bar{N}_j H + M_{ij} \bar{N}_i \bar{N}_j, \tag{2.7}$$

where Ψ_i are **10**-dimensional multiplets, Φ_i are **5**-dimensional ones, N_i denote the right-handed neutrino superfields, and H ($\bar{H}$) is **5**- ($\bar{\mathbf{5}}$-) dimensional Higgs multiplets. i and j mean the generation of the fermions, $i, j = 1, 2, 3$. f^u, f^d, and f^ν are Yukawa coupling matrices for the up-type quarks, down-type quarks (charged leptons) and neutrinos, respectively. These are given by

$$f^u_{ij} = V_{ki} f_{u_k} e^{i\varphi_{u_k}} V_{kj}, \tag{2.8}$$

$$f^d_{ij} = f_{d_i} \delta_{ij}, \tag{2.9}$$

$$f^\nu_{ij} = e^{i\varphi_{d_i}} U^*_{ij} f_{\nu_j}, \tag{2.10}$$

without a loss of generality, where V and U are the Cabibbo-Kobayashi-Maskawa (CKM) and Pontecorvo-Maki-Nakagawa-Sakata (PMNS) matrices, respectively. φ_{u_k} and φ_{d_i} are CP-violating phases, and f_{u_k} and f_{d_i} are Yukawa couplings of the up- and down-type quarks (charged leptons), respectively. For the neutrinos sector, the light neutrino masses are given by the seesaw mechanism $m_{\nu_i} = f^2_{\nu_i} v_u^2 / M_{N_i}$, where v_u is the vacuum expectation value (VEV) of the up-type Higgs in H, and M_{N_i} are the mass eigenvalues of the right-handed neutrinos. Here, we assume a diagonal right-handed Majorana mass matrix M_{ij} for simplicity.

JHEP03(2015)160

2.1.2 Photon polarization in SUSY SU(5) with right-handed neutrino

We discuss C_7 and C_7', which determine the magnitude of the photon polarization, in the model of SUSY SU(5) GUT with N_R. In supersymmetric models, the dominant contributions to $C_{7,8}$ and $C_{7,8}'$ arise from loop diagrams of the charged Higgses, charginos, and gluinos. Thus, $C_{7,8}^{\rm NP} = C_{7,8}^{H^\pm} + C_{7,8}^{\tilde\chi^\pm} + C_{7,8}^{\tilde g}$ and $C_{7,8}'^{\rm NP} = C_{7,8}'^{H^\pm} + C_{7,8}'^{\tilde\chi^\pm} + C_{7,8}'^{\tilde g}$ in the SUSY SU(5) model with N_R where $C_{7,8}^{H^\pm}$ ($C_{7,8}'^{H^\pm}$), $C_{7,8}^{\tilde\chi^\pm}$ ($C_{7,8}'^{\tilde\chi^\pm}$), and $C_{7,8}^{\tilde g}$ ($C_{7,8}'^{\tilde g}$) are the contributions to $C_{7,8}$ ($C_{7,8}'$) from the charged Higgses, charginos, and gluinos, respectively. These contributions are calculated as [18]

$$C_7^{H^\pm} = C_7'^{H^\pm} \simeq \left(\frac{1-\epsilon t_\beta}{1+\epsilon t_\beta}\right)\frac{1}{2}h_7(y_t), \tag{2.11}$$

$$C_7^{\tilde\chi^\pm} = \frac{4G_F}{\sqrt{2}}\frac{g_2^2}{\tilde m^2}\left[\frac{(\delta_u^{LL})_{32}}{V_{tb}V_{ts}^*}\frac{\mu M_2}{\tilde m^2}f_7^{(1)}(x_2,x_\mu) + \frac{m_t^2}{M_W^2}\frac{A_t\mu}{\tilde m^2}f_7^{(2)}(x_\mu)\right]\frac{t_\beta}{1+\epsilon t_\beta}, \tag{2.12}$$

$$C_7'^{\tilde\chi^\pm} = \frac{4G_F}{\sqrt{2}}\frac{g_2^2}{\tilde m^2}\left[\frac{(\delta_u^{RR})_{32}}{V_{tb}V_{ts}^*}\frac{\mu M_2}{\tilde m^2}f_7^{(1)}(x_2,x_\mu) + \frac{m_t^2}{M_W^2}\frac{A_t\mu}{\tilde m^2}f_7^{(2)}(x_\mu)\right]\frac{t_\beta}{1+\epsilon t_\beta}, \tag{2.13}$$

$$C_7^{\tilde g^\pm} = \frac{4G_F}{\sqrt{2}}\frac{g_s^2}{\tilde m^2}\left[\frac{M_{\tilde g}}{m_b}\frac{(\delta_d^{RL})_{32}}{V_{tb}V_{ts}^*}g_7^{(1)}(x_g) + \frac{M_{\tilde g}\mu}{\tilde m^2}\frac{t_\beta}{1+\epsilon t_\beta}\frac{(\delta_d^{LL})_{32}}{V_{tb}V_{ts}^*}g_7^{(2)}(x_g)\right], \tag{2.14}$$

$$C_7'^{\tilde g^\pm} = \frac{4G_F}{\sqrt{2}}\frac{g_s^2}{\tilde m^2}\left[\frac{M_{\tilde g}}{m_b}\frac{(\delta_d^{LR})_{32}}{V_{tb}V_{ts}^*}g_7^{(2)}(x_g) + \frac{M_{\tilde g}\mu^*}{\tilde m^2}\frac{t_\beta}{1+\epsilon t_\beta}\frac{(\delta_d^{RR})_{32}}{V_{tb}V_{ts}^*}g_7^{(1)}(x_g)\right], \tag{2.15}$$

and

$$C_8^{H^\pm} = C_8'^{H^\pm} \simeq \left(\frac{1-\epsilon t_\beta}{1+\epsilon t_\beta}\right)\frac{1}{2}h_8(y_t), \tag{2.16}$$

$$C_8^{\tilde\chi^\pm} = \frac{4G_F}{\sqrt{2}}\frac{g_2^2}{\tilde m^2}\left[\frac{(\delta_u^{LL})_{32}}{V_{tb}V_{ts}^*}\frac{\mu M_2}{\tilde m^2}f_8^{(1)}(x_2,x_\mu) + \frac{m_t^2}{M_W^2}\frac{A_t\mu}{\tilde m^2}f_8^{(2)}(x_\mu)\right]\frac{t_\beta}{1+\epsilon t_\beta}, \tag{2.17}$$

$$C_8'^{\tilde\chi^\pm} = \frac{4G_F}{\sqrt{2}}\frac{g_2^2}{\tilde m^2}\left[\frac{(\delta_u^{RR})_{32}}{V_{tb}V_{ts}^*}\frac{\mu M_2}{\tilde m^2}f_8^{(1)}(x_2,x_\mu) + \frac{m_t^2}{M_W^2}\frac{A_t\mu}{\tilde m^2}f_8^{(2)}(x_\mu)\right]\frac{t_\beta}{1+\epsilon t_\beta}, \tag{2.18}$$

$$C_8^{\tilde g^\pm} = \frac{4G_F}{\sqrt{2}}\frac{g_s^2}{\tilde m^2}\left[\frac{M_{\tilde g}}{m_b}\frac{(\delta_d^{RL})_{32}}{V_{tb}V_{ts}^*}g_8^{(1)}(x_g) + \frac{M_{\tilde g}\mu}{\tilde m^2}\frac{t_\beta}{1+\epsilon t_\beta}\frac{(\delta_d^{LL})_{32}}{V_{tb}V_{ts}^*}g_8^{(2)}(x_g)\right], \tag{2.19}$$

$$C_8'^{\tilde g^\pm} = \frac{4G_F}{\sqrt{2}}\frac{g_s^2}{\tilde m^2}\left[\frac{M_{\tilde g}}{m_b}\frac{(\delta_d^{LR})_{32}}{V_{tb}V_{ts}^*}g_8^{(2)}(x_g) + \frac{M_{\tilde g}\mu^*}{\tilde m^2}\frac{t_\beta}{1+\epsilon t_\beta}\frac{(\delta_d^{RR})_{32}}{V_{tb}V_{ts}^*}g_8^{(1)}(x_g)\right], \tag{2.20}$$

at the weak scale and $\epsilon \simeq \alpha_s/(3\pi) \sim \mathcal{O}(10^{-2})$ for a degenerate SUSY spectrum, $t_\beta = \tan\beta \equiv v_u/v_d$, v_d is the VEV of down-type Higgs, g_2 is the $SU(2)_L$ gauge coupling constant, $\tilde m$ is an averaged squark mass, $(\delta_q^{XY})_{ij}$ ($q = u, d$ and $X, Y = L, R$) are mass insertion parameters, μ is the supersymmetric Higgs mass, M_x ($x = 2, \tilde g$) are the gaugino masses, and A_t is the soft scalars coupling for the top quark. $h_{7,8}$, $f_{7,8}^{(1,2)}$, and $g_{7,8}^{(1,2)}$ are loop functions, which are given in appendix A. The mass insertion parameters are given in appendix B. And, we define $y_t \equiv m_t^2/M_{H^\pm}^2$, $x_2 \equiv |M_2|^2/\tilde m^2$, $x_\mu \equiv |\mu|^2/\tilde m^2$, and $x_g \equiv M_{\tilde g}^2/\tilde m^2$ where m_t and $M_{H^\pm}$ are the top quark and charged Higgs masses, respectively. The contributions from the charged Higgs and chargino to $C_7'^{\rm NP}$ are suppressed by m_s/m_b.

In order to see the magnitude of contributions from NP, we estimate the ratio $|C_7'/C_7|$ at the b quark mass scale, which determines the size of polarization of photon as seen

JHEP03(2015)160

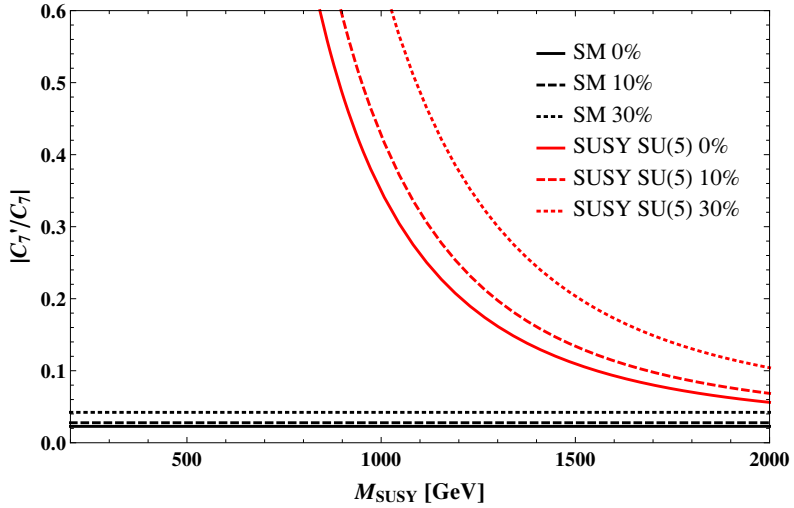

Figure 1. The magnitude of $|C_7'/C_7|$ in the SM and SUSY SU(5) GUT with N_R which are depicted by the black and red curves, respectively. The contours with $n\%$ correspond to cases that there is $n\%$ misidentification in the C_7 measurement at experiments, i.e. each of the contours denotes $|C_7'(1+n/100)/(C_7(1-n/100))|$.

below. The value of the ratio in the model of SUSY SU(5) GUT with N_R is shown by the red solid curve in figure 1. The black solid line indicates the SM case $|C_7'^{\rm SM}/C_7^{\rm SM}|$ which can be approximated as $|C_7'^{\rm SM}/C_7^{\rm SM}| \simeq m_s/m_b$. One can see that $|C_7'/C_7|$ in the SUSY SU(5) with N_R case is enhanced from the SM. This means that the final state of s_R in $b \to s\gamma$ increases compared to the SM while the most of final state of $b \to s\gamma$ in the SM is s_L due to the suppression proportional to m_s/m_b.

In figure 1, the horizontal axis is a typical scale of NP, which is a SUSY breaking scale $M_{\rm SUSY}$ in the SUSY SU(5) GUT with N_R case. One can see that at a large limit of $M_{\rm SUSY}$, the ratio $|C_7'/C_7|$ closes to the SM case, $|C_7'/C_7| \to |C_7'^{\rm SM}/C_7^{\rm SM}|$. The contours with $n\%$ correspond to case that there is $n\%$ misidentification in the C_7 measurement at experiments, i.e. the contours denote $|C_7'(1+n/100)/(C_7(1-n/100))|$. This misidentification corresponds to a mismatch in the conversion of left-handed helicity to the left-handed chirality. (The helicity is determined in experiments.) For instance, if one identifies the left-handed helicity with the left-handed chirality with 10% misidentification, the right-handed chirality is over estimated as 110% of the true value. Thus, the contours go above as n increases in figure 1. In the calculation, we take

$$
\begin{aligned}
&t_\beta = 10, && M_{\rm SUSY} = m_{1/2}, && m_0 = A_0 = A_t = A_b = 1\,{\rm TeV},\\
&\mu = 1.01 m_0, && M_2 = 0.822 M_{\rm SUSY}, && M_{\tilde g} = 2.86 M_{\rm SUSY},\\
&M_{H_c} = 10^{16}\,{\rm GeV}, && \tilde m_{\tilde u}^2 = \sqrt{m_{\tilde Q_L}^2\, m_{\tilde u_R}^2}, && \tilde m_{\tilde d}^2 = \sqrt{m_{\tilde Q_L}^2\, m_{\tilde d_R}^2},\\
&m_{\tilde Q_L}^2 = m_0^2 + 6.86 M_{\rm SUSY}^2, && m_{\tilde u_R}^2 = m_0^2 + 6.44 M_{\rm SUSY}^2, && m_{\tilde d_R}^2 = m_0^2 + 6.39 M_{\rm SUSY}^2,\\
&f_{\nu_i} = 1, && \varphi_{u_{23}} = 0.01, && \varphi_{d_{23}} = \pi,
\end{aligned}
\tag{2.21}
$$

JHEP03(2015)160

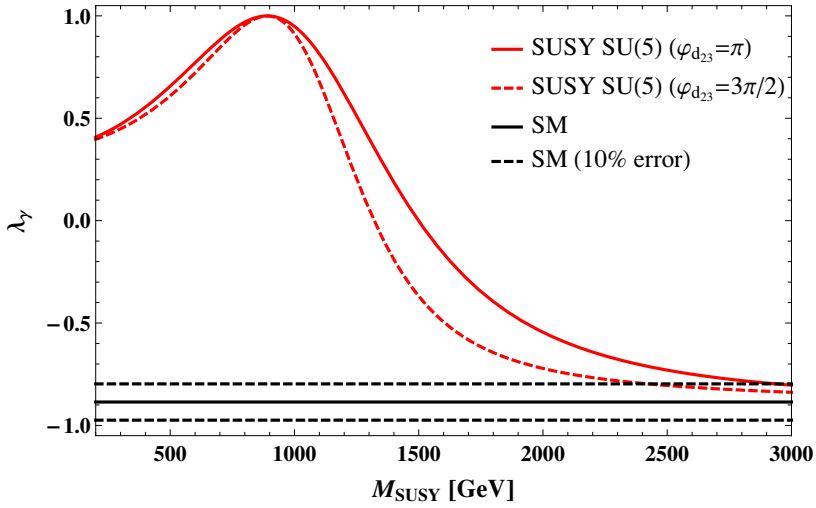

Figure 2. The polarization parameter λ_γ in $b \to s\gamma$ in the SM and SUSY SU(5) GUT with N_R which are depicted by the black and red curves, respectively. We also show $\varphi_{d_{23}} = 3\pi/2$ case by the red dashed curve and 10% error in the SM prediction by the black dashed curve for comparison.

as a typical point where CP phases are given in the radian unit.[2] We take other values of parameters in the SM and the neutrino sector (PMNS mixing angles) as the best fit values given in [19, 20].

Next, we consider the polarization parameter of photon λ_γ at the b quark mass scale defined as

$$\lambda_\gamma \equiv \frac{\mathrm{Re}[C_7'/C_7]^2 + \mathrm{Im}[C_7'/C_7]^2 - 1}{\mathrm{Re}[C_7'/C_7]^2 + \mathrm{Im}[C_7'/C_7]^2 + 1}. \tag{2.22}$$

In order to measure λ_γ we need to consider a parity-odd observable in the $B_d \to X_s\gamma$ decay since the photon polarization is parity-odd. In refs. [4, 5] they proposed that λ_γ can be measured from the up-down asymmetry of the photon direction relative to the $K\pi\pi$ decay plane in the $K_1(1400)$ rest frame. We show λ_γ in figure 2 and the SM and SUSY SU(5) GUT with N_R cases are depicted by the black and red curves, respectively. We also show $\varphi_{d_{23}} = 3\pi/2$ case by the red dashed curve for comparison. The SM prediction for the photon polarization still have roughly 10% error due to $\mathcal{O}_2$ operator [11], then we depict it by the black dashed curve.

The superKEKB with an integrated luminosity of 75 ab^{-1} and the LHCb with 2 fb^{-1} might reach the 20 ($|\lambda_\gamma| = 0.8|\lambda_\gamma^{\rm SM}|$) and 10% ($|\lambda_\gamma| = 0.9|\lambda_\gamma^{\rm SM}|$) precision, respectively [11, 21]. Thus, the future experiment will be able to check the NP scale up to about 1700 GeV (which corresponds to $M_2 \simeq 1400$ GeV and $M_{\tilde{g}} \simeq 4900$ GeV) in this model of SUSY SU(5) with N_R.

[2]Note that $\varphi_{d_{23}}$ is sensitive to the CEDM. The allowed minimal and maximal values by the CEDM constraint are π and $3\pi/2$ (or $\pi/2$), respectively. In the calculation of photon polarization, we take the minimal value. The photon polarization is not so sensitive to the value of $\varphi_{d_{23}}$ but the difference between these values appears in the calculation of direct CP asymmetry as we will show in section 3. We have numerically checked that another phase, $\varphi_{u_{23}}$, is not sensitive to our evaluation.

JHEP03(2015)160

2.2 Case of Left-right symmetric standard model

2.2.1 Model

Next, we consider the case in the left-right symmetric standard model (LRSM) [22–25]. The model is based on the gauge group $\mathrm{SU}(2)_L \times \mathrm{SU}(2)_R \times \mathrm{U}(1)_{\tilde{Y}}$. In the model, the SM left-handed doublet fermions are $\mathrm{SU}(2)_R$ singlets, and the right-handed fermions including the neutrinos are $\mathrm{SU}(2)_R$ doublets and $\mathrm{SU}(2)_L$ singlets. For the Higgs sector, the model includes a bi-doublet scalar Φ under the $\mathrm{SU}(2)_L \times \mathrm{SU}(2)_R$ transformation, an $\mathrm{SU}(2)_R$ triplet Δ_R, and an $\mathrm{SU}(2)_L$ triplet Δ_L in order to realize a realistic symmetry breaking, $\mathrm{SU}(2)_L \times \mathrm{SU}(2)_R \times \mathrm{U}(1)_{\tilde{Y}} \to \mathrm{SU}(2)_L \times \mathrm{U}(1)_Y \to \mathrm{U}(1)_{\mathrm{em}}$. The symmetry breaking can be undertaken by the VEVs of Φ, Δ_R, and Δ_L as

$$\langle \Phi \rangle = \begin{pmatrix} \kappa & 0 \\ 0 & \kappa' e^{i\omega} \end{pmatrix}, \quad \langle \Delta_R \rangle = \begin{pmatrix} 0 & 0 \\ v_R & 0 \end{pmatrix}, \quad \langle \Delta_L \rangle = \begin{pmatrix} 0 & 0 \\ v_L e^{i\theta_L} & 0 \end{pmatrix}, \tag{2.23}$$

with six real numbers κ, κ', ω, v_R, v_L, and θ_L. Regarding the magnitude of the VEVs, v_R should be much larger than the electroweak (EW) scale to suppress the right-handed currents at low energy, and the EW ρ-parameter limits v_L to be $v_L \lesssim 10$ GeV [26]. In this work, we take $v_L = 0$ for simplicity, which is usually taken in literatures (e.g., [27, 28]). Since the VEV of Φ leads to the standard EW symmetry breaking, we define $v \equiv \sqrt{\kappa^2 + \kappa'^2} = 174\,\mathrm{GeV}$, $\tan\beta_{\mathrm{LR}} \equiv \kappa/\kappa'$, and $\epsilon_{\mathrm{LR}} \equiv v/v_R$.

The charged gauge bosons are given by the admixture of the mass eigenstates as

$$\begin{pmatrix} W_L^- \\ W_R^- \end{pmatrix} = \begin{pmatrix} \cos\zeta & -\sin\zeta e^{i\omega} \\ \sin\zeta e^{i\omega} & \cos\zeta \end{pmatrix} \begin{pmatrix} W_1^- \\ W_2^- \end{pmatrix}. \tag{2.24}$$

The masses of charged gauge bosons are approximated as

$$M_{W_1} \simeq \frac{g_L v}{\sqrt{2}}(1 - \epsilon_{\mathrm{LR}}^2 \sin^2\beta_{\mathrm{LR}} \cos^2\beta_{\mathrm{LR}}), \quad M_{W_2} \simeq g_R v_R \left(1 + \frac{1}{4}\epsilon_{\mathrm{LR}}^2\right), \tag{2.25}$$

where $g_{L,R}$ are the gauge couplings of $\mathrm{SU}(2)_{L,R}$ and we take $g_R/g_L = 1$ for simplicity in the numerical analysis. The mixing angle is given as $\sin\zeta \approx (M_{W_1}^2/M_{W_2}^2)\sin 2\beta_{LR}$. M_{W_2} is identified with M_{NP} in the LRSM. There are also charged and heavy neutral Higgs bosons in the LRSM. And their masses are nearly the same, $M_{H^\pm} \simeq M_{H^0} \simeq M_{A^0}$, where $M_{H^\pm}$ are the masses of the charged Higgs bosons and M_{H^0,A^0} are the neutral Higgs bosons masses [27, 29]. In this work, we represent both the charged and neutral Higgs bosons masses as M_H for simplicity. Regarding the flavor mixing matrices, we assume $V = V_L = V_R$, where V_L and V_R are the mixing matrices for the left- and right-handed quarks, respectively. $V = V_L = V_R$ is taken in the so-called the manifest LRSM [30, 31] and we also take the equality in this work. In our numerical analyses, we have three free parameters, i.e. M_H, $M_{\mathrm{NP}} = M_{W_2}$, and $\tan\beta_{\mathrm{LR}}$.[3]

[3]The value of M_{W_2} is not exactly determined even if one takes $g_R/g_L = 1$ and fixes the value of M_H, because the heavy Higgs masses depend on scalar quartic couplings, which can be in region from 0 to 4π, and/or trilinear couplings. Thus, one can generally take both M_{W_2} and M_H as free parameters in this model.

JHEP03(2015)160

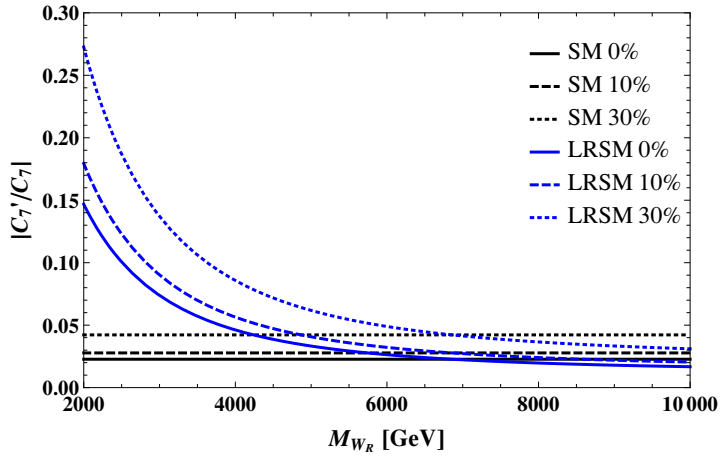

Figure 3. The magnitude of $|C_7'/C_7|$ in the SM and LRSM which are depicted by the black and blue curves, respectively. The meaning of each contour is the same as figure 1.

2.2.2 Photon polarization in LRSM

$C_7^{\rm NP}$ and $C_7'^{\rm NP}$ in the LRSM are generally given by

$$\begin{aligned}
C_7^{\rm NP} =& -\sin^2\zeta\left(D_0'(x_t)-\frac{M_{W_1}^2}{M_{W_2}^2}D_0'(\tilde{x}_t)\right)\\
&+\frac{m_t}{m_b}\frac{g_R}{g_L}\frac{V_{tb}^R}{V_{tb}}\sin\zeta\cos\zeta e^{i\omega}\left(A_{\rm LR}(x_t)-\frac{M_{W_1}^2}{M_{W_2}^2}A_{\rm LR}(\tilde{x}_t)\right)\\
&+\frac{m_c}{m_b}\frac{g_R}{g_L}\frac{V_{cs}^*V_{cb}^R}{V_{ts}^*V_{tb}}\sin\zeta\cos\zeta e^{i\omega}\left(A_{\rm LR}(x_c)-\frac{M_{W_1}^2}{M_{W_2}^2}A_{\rm LR}(\tilde{x}_c)\right)+\frac{m_t}{m_b}\frac{\tan(2\beta_{\rm LR})}{\cos(2\beta_{\rm LR})}e^{i\omega}\frac{V_{tb}^R}{V_{tb}}h_7(y)\\
&+\tan(2\beta_{\rm LR})A_H^2(x), \qquad (2.26)\\
C_7'^{\rm NP} =& \frac{g_R^2}{g_L^2}\frac{V_{ts}^{R*}V_{tb}^R}{V_{ts}^*V_{tb}}\left(\sin^2\zeta D_0'(x_t)+\cos^2\zeta\frac{M_{W_1}^2}{M_{W_2}^2}D_0'(\tilde{x}_t)\right)\\
&+\frac{m_t}{m_b}\frac{g_R}{g_L}\frac{V_{ts}^{R*}}{V_{ts}^*}\sin\zeta\cos\zeta e^{-i\omega}\left(A_{\rm LR}(x_t)-\frac{M_{W_1}^2}{M_{W_2}^2}A_{\rm LR}(\tilde{x}_t)\right)\\
&+\frac{m_c}{m_b}\frac{g_R}{g_L}\frac{V_{cs}^{R*}V_{cb}}{V_{ts}^*V_{tb}}\sin\zeta\cos\zeta e^{-i\omega}\left(A_{\rm LR}(x_c)-\frac{M_{W_1}^2}{M_{W_2}^2}A_{\rm LR}(\tilde{x}_c)\right)\\
&+\frac{m_t}{m_b}\frac{\tan(2\beta_{\rm LR})}{\cos(2\beta_{\rm LR})}e^{-i\omega}\frac{V_{ts}^{R*}}{V_{ts}^*}h_7(y)+\frac{V_{ts}^{R*}V_{tb}^R}{V_{ts}^*V_{tb}}\frac{1}{\cos^2(2\beta_{\rm LR})}A_H^2(x), \qquad (2.27)
\end{aligned}$$

when one does not assume $g_R/g_L = 1$ and $V = V_R$, where loop functions $D_0'(x)$ and $A_{\rm LR}(x)$ are given in appendix A, and $x_t \equiv m_t^2/m_{W_1}^2$, $\tilde{x}_t \equiv m_t^2/m_{W_2}^2$, $x_c \equiv m_c^2/m_{W_1}^2$, $\tilde{x}_c \equiv m_c^2/m_{W_2}^2$, and $y \equiv m_t^2/M_H^2$. The ratio $|C_7'/C_7|$ in the LRSM is shown by the blue curves in figure 3. The value of the ratio in the LRSM is larger than the both cases of SM and SUSY SU(5) with N_R model because the right-handed current in the LRSM is more effective than those

JHEP03(2015)160

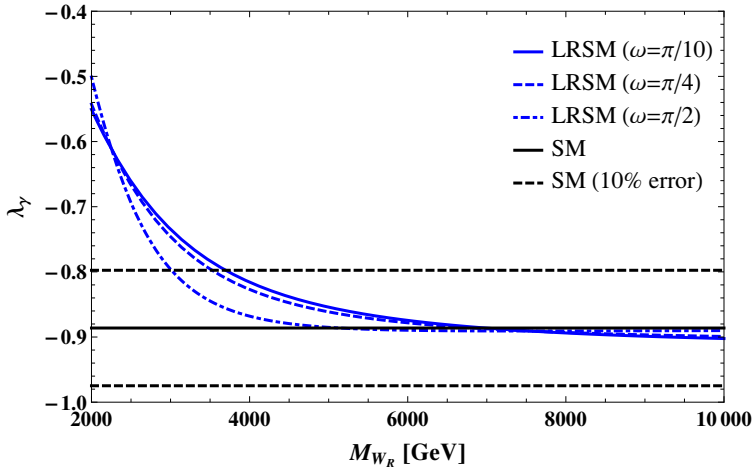

Figure 4. The polarization parameter λ_γ in $b \to s\gamma$ in the SM and LRSM which are depicted by the black and blue curves, respectively. We also show $\omega = \pi/4$ and $\pi/2$ cases by the blue dashed and dashed-dotted curves for comparison, respectively.

models. In the analysis, we take

$$\frac{g_R}{g_L} = 1, \quad V = V^R, \quad \tan\beta_{\rm LR} = 10, \quad \omega = \frac{\pi}{10}, \quad M_{H^\pm} = 15{\rm TeV}, \tag{2.28}$$

as a sample point.[4]

The polarization parameter in the LRSM is shown by the blue curve in figure 4. The SM and LRSM cases are depicted by the black and blue curves, respectively. We also show $\omega = \pi/4$ and $\pi/2$ cases by the blue dashed and dashed-dotted curves for comparison, respectively. Since $M_{\rm NP} \simeq 3.7\,{\rm TeV}$ for 10 % deviation from the SM prediction, the future LHCb experiment with $2\,{\rm fb}^{-1}$ will check the scale of the right-handed gauge boson up to 3.7 TeV in this case. The dependence of photon polarization on the CP phase is not strong.

3 CP asymmetry

Next, we evaluate the CP asymmetry in $b \to s\gamma$ process in each model. The CP asymmetry can be categorized into two parts: one is the direct CP asymmetry which is induced by the CP phase in the decay amplitude, and the other is the time-dependent CP asymmetry which is induced during the meson mixing.

3.1 Direct CP asymmetry

In addition to the determination of photon polarization, the observation of CP asymmetry in the $b \to s\gamma$ process is still sensitive to the existence of NP. Thus, we evaluate the CP asymmetry of the process in both models of SUSY SU(5) GUT with N_R and LRSM. The

[4]Although there are crossing points of the NP lines with the SM prediction line in all figures afterward, they are due to the fixing of the charged Higgs mass.

JHEP03(2015)160

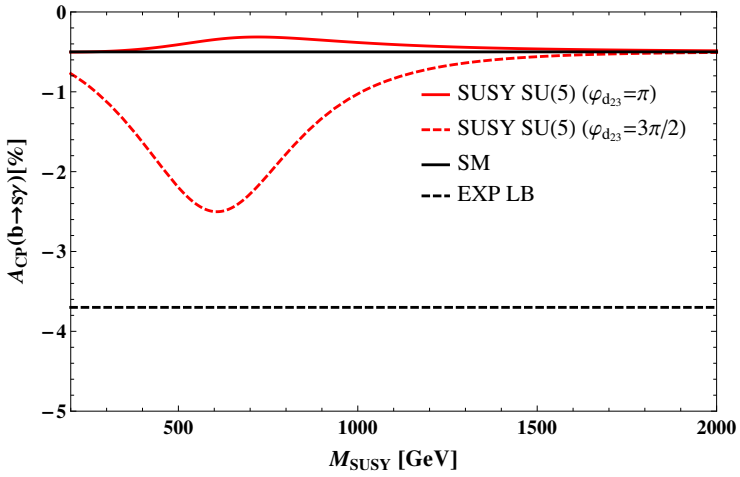

Figure 5. The direct CP asymmetry in $b \to s\gamma$ in the SM and SUSY SU(5) GUT with N_R, which are depicted by the black and red solid curves. The black dashed line corresponds to the current experimental lower bound [33]. We also show the $\varphi_{d_{23}} = 3\pi/2$ case by the red dashed curve for comparison.

asymmetry is given by

$$\begin{aligned} A_{\rm CP}(b\to s\gamma) &\equiv \frac{\Gamma(B\to X_{\bar{s}}\gamma)-\Gamma(\bar{B}\to X_s\gamma)}{\Gamma(B\to X_{\bar{s}}\gamma)+\Gamma(\bar{B}\to X_s\gamma)} \\ &\simeq -\frac{1}{|C_7|^2+|C_7'|^2}(1.23\ {\rm Im}[C_2C_7^*]-9.52\ {\rm Im}[C_8C_7^*+C_8'C_7'^*]+0.10\ {\rm Im}[C_2C_8^*]) \\ &\quad -0.5 \quad (\text{in } \%), \end{aligned} \tag{3.1}$$

which of course strongly depends on the CP-phases in the model where C_2 is the coefficient of the operator $O_2 = (\bar{c}^\alpha\gamma_\mu P_L b^\alpha)(\bar{c}^\beta\gamma^\mu P_L b^\beta)$ in the effective Hamiltonian of $\Delta F = 2$ transitions. Note that the contributions from NP to C_2 and C_2' are negligibly small while $C_{7,8}$ and $C_{7,8}'$ include contributions from NP, i.e. $C_2' \ll C_2 = C_2^{\rm SM} = 1$. Thus, $A_{\rm CP}(b\to s\gamma)$ is well approximated by eq. (3.1).[5]

3.1.1 SUSY SU(5) with right-handed neutrino case

We show $A_{\rm CP}(b\to s\gamma)$ in the SUSY SU(5) with N_R and SM cases by red and black solid curves in figure 5, respectively. The experimental lower bound as -3.7 % [19] is also shown by the black dashed line. We also show $\varphi_{d_{23}} = 3\pi/2$ case by the red dashed curve for comparison. It turns out that the magnitude of the direct CP asymmetry in the case of SUSY SU(5) with N_R highly depend on the phase $\varphi_{d_{23}}$. The current experimental lower bound does not constrain the scale of NP, $M_{\rm SUSY}$ in this parameter setup. Therefore, the measurement of $A_{\rm CP}$ does not currently constrain on the NP scale in the SUSY SU(5) with N_R model even if one takes the maximally allowed CP phase as $\varphi_{d_{23}} = 3\pi/2$. But, the expected reach of Belle II with 50 ab^{-1} for $A_{\rm CP}(B\to X_{s+d}\gamma)$ will be $\pm 2\%$ precision. Thus,

[5]There is also an error in the SM prediction but it is enough small [32]. Therefore, we neglect such correction here just for simplicity.

JHEP03(2015)160

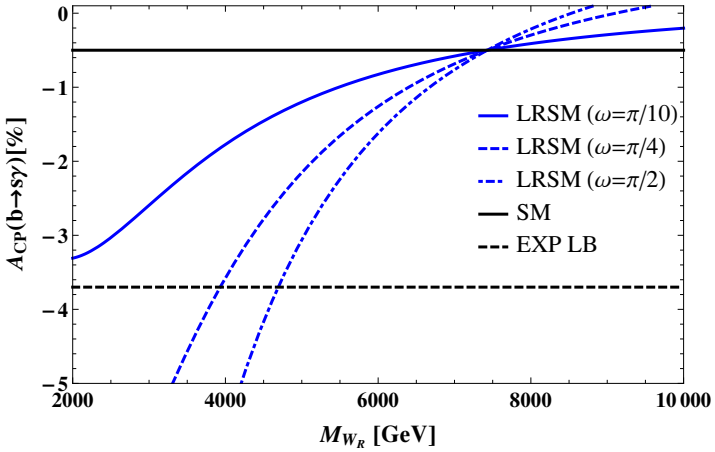

Figure 6. The direct CP asymmetry in $b \to s\gamma$ in the SM and LRSM which are depicted by the black and blue solid curves. The black dashed line is same as in figure 5. We also show $\omega = \pi/4$ and $\pi/2$ cases by the blue dashed and dashed-dotted curves for comparison, respectively.

the future determination will check NP between 450-750 GeV in this typical SUSY SU(5) with N_R case.

3.1.2 LRSM case

For the LRSM, $C_8^{\rm NP}$ and $C_8'^{\rm NP}$ are

$$C_8 = \rho_8 \Delta^{LR} C_8 + \rho_{\rm LR} \frac{m_c}{m_b} \sin\zeta \cos\zeta e^{i\alpha} \frac{V_{cb}^R}{V_{cb}^L}\,, \tag{3.2}$$

$$C_8' = \rho_8 \Delta^{LR} C_8' + \rho_{\rm LR} \frac{m_c}{m_b} \sin\zeta \cos\zeta e^{-i\alpha} \frac{V_{cb}^{R*}}{V_{cb}^{L*}}\,, \tag{3.3}$$

with

$$\Delta^{LR} C_8 = \frac{m_t}{m_b} \sin\zeta \cos\zeta e^{i\alpha} \frac{V_{tb}^R}{V_{tb}^L} f_{\rm LR}(\tilde{x}_t)\,, \tag{3.4}$$

$$\Delta^{LR} C_8' = \frac{m_t}{m_b} \sin\zeta \cos\zeta e^{-i\alpha} \frac{V_{ts}^{R*}}{V_{ts}^{L*}} f_{\rm LR}(\tilde{x}_t)\,, \tag{3.5}$$

where ρ_8 and $\rho_{\rm LR}$ are the so-called magic number which are given in the ref. [27]. $f_{\rm LR}(x)$ is also a loop function for the left-right symmetric model given in appendix A.

The asymmetry in the LRSM is shown by the blue curve in figure 6. We also show $\omega = \pi/4$ and $\pi/2$ cases by the blue dashed and dashed-dotted curves for comparison, respectively. One can see from figure 6 that the magnitude of the direct CP asymmetry in the LRSM is allowed for $M_{\rm NP} \geq 2\,$TeV for $\pi/10$. Hence, the $A_{\rm CP}$ measurement does not give constraint on the existence of NP in this case at the moment. Furthermore, the future Belle II with 50 ab^{-1} will check the LRSM model up to 3.5TeV, 5TeV, and 5.5TeV for $\omega = \pi/10$, $\omega = \pi/4$, and $\omega = \pi/2$, respectively. The result is really sensitive to the phase ω as with SUSY SU(5) with N_R case.

JHEP03(2015)160

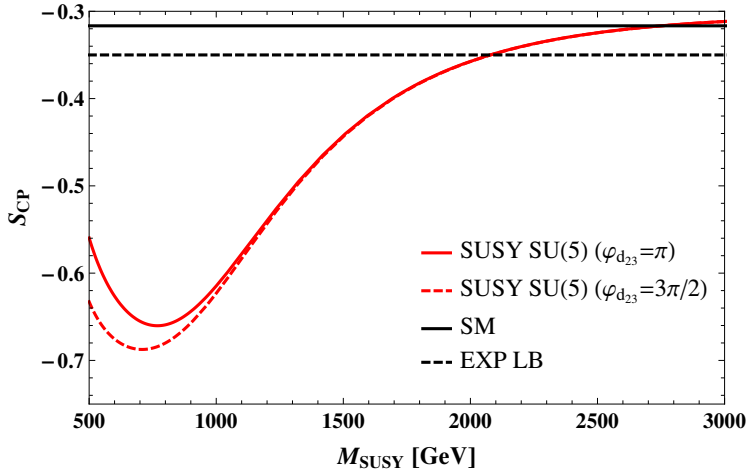

Figure 7. The time-dependent CP asymmetry in $B \to K_s\pi^0\gamma$ in the SM and SUSY SU(5) GUT with N_R, which are depicted by the black and blue solid curves. The black dashed line is the current experimental lower bound [33]. We also show $\varphi_{d_{23}} = 3\pi/2$ case by the red dashed curve for comparison.

3.2 Time-dependent CP asymmetry

We also evaluate the time-dependent CP asymmetry in the $B \to K_s\pi^0\gamma$ decay denoted as S_{CP}. The definition of S_{CP} is same in the both model:

$$S_{\rm CP} = 2\frac{{\rm Im}\left[e^{-2i\beta_{CKM}}C_7C_7'\right]}{|C_7|^2+|C_7'|^2}, \tag{3.6}$$

where $2\beta_{CKM} \approx 43^\circ$ is a CP phase in $B \to K_s\pi^0\gamma$ decay.

3.2.1 SUSY SU(5) with right-handed neutrino case

We show eq. (3.6) in the SUSY SU(5) with N_R and SM cases by red and black solid curves in figure 7, respectively. The current experimental lower bound as -0.35 is also shown by the black dashed line. We also show $\varphi_{d_{23}} = 3\pi/2$ case by the red dashed curve for comparison. The current experimental bound seems to exclude up to 2 TeV of the $M_{\rm SUSY}$ in figure 7 in this naive set up. In other words, the time-dependent CP asymmetry gives the strongest constraint within λ_γ, $A_{\rm CP}$, and $S_{\rm CP}$.

3.2.2 LRSM case

We show eq. (3.6) in the LRSM and SM cases by blue and black solid curves in figure 8, respectively. The current experimental lower bound constrains the mass of W_R up to 7 TeV in this simple set up. The figure shows that the time-dependent CP asymmetry is the strongest constraint even in the LRSM.

JHEP03(2015)160

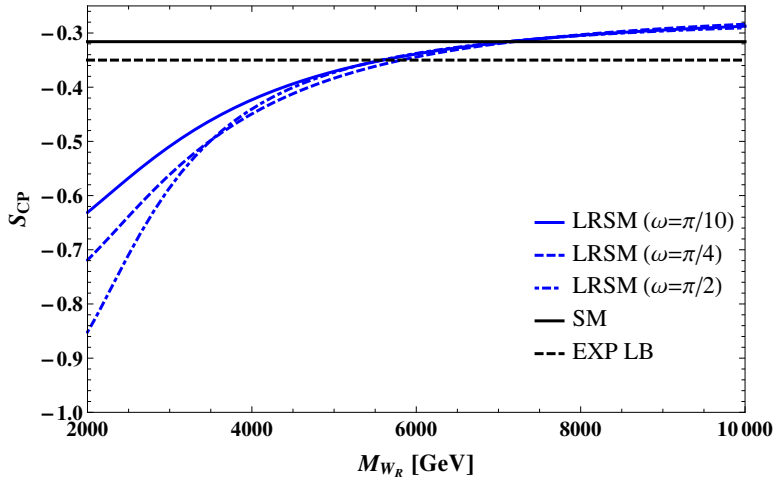

Figure 8. The time-dependent CP asymmetry in $B \to K_s\pi^0\gamma$ in the SM and LRSM which are depicted by the black and blue solid curves. The black dashed line is same as in figure 7. We also show $\omega = \pi/4$ and $\pi/2$ cases by the blue dashed and dashed-dotted curves for comparison, respectively.

4 Comparison between Photon polarization and Measurements of CP asymmetry

As we mentioned in the Introduction, the photon polarization might become a useful way to determine NP. Actually, the ways to determine the photon chirality by measurement of angular distribution of the final state particles have been discussed in several papers [9–11] (See also [34, 35]). In this paper, we have evaluated three observables: photon polarization, direct CP asymmetry, and time-dependent CP asymmetry. We give some comments on the comparison among the results of those:

- For the determination of photon polarization in the SUSY SU(5) with N_R model, the future LHCb experiment with $2\,\text{fb}^{-1}$ will be able to check the NP scale up to about 1700 GeV, which corresponds to $M_2 \simeq 1400\,\text{GeV}$ and $M_{\tilde{g}} \simeq 4900\,\text{GeV}$, at the typical point of this model.

- For the measurement of A_{CP} in the SUSY SU(5) with N_R model, the experiment does not currently constrain on the NP scale even if one takes the maximally allowed CP phase as $\varphi_{d_{23}} = 3\pi/2$. The future Belle II with 50 ab^{-1} will check NP between 450–750 GeV.

- For the determination of photon polarization in the LRSM, the future LHCb experiment will check the NP scale up to 3.7 TeV in this case.

- For the measurement of A_{CP} in the LRSM, the experiment constrain up to 4.7 TeV depending on the phase ω. Furthermore, the future Belle II with 50 ab^{-1} will check up to 5.5 TeV when ω maximize the direct CP asymmetry. On the other hand, the future experiment reach 3.5 TeV at most when ω minimize the direct CP asymmetry.

JHEP03(2015)160

- The time-dependent CP asymmetry is the most stringent constraint in both models and this CP asymmetry does not depend on CP asymmetry parameters so much.
- Thus, we mention that there is a region where the determination of photon polarization is more ascendant for the NP search than that of direct CP asymmetry in both models. However, time-dependent CP asymmetry always gives us more stringent constraint than other observables.

5 Summary

One might be able to obtain the existence of NP and discriminate among the SM and NP if one can precisely determine the chirality of the s quark in the $b \to s\gamma$ process. The chirality of s quark can be determined by measuring the polarization of photon in the process. And, there are several ways to measure the photon polarization. In addition to the determination of photon polarization, the observation of CP asymmetry in the process is still sensitive to the existence of NP. Thus, simultaneous studies of photon polarization and CP asymmetry in the $b \to s\gamma$ process will be intriguing for the experimental search of NP.

We have investigated the $b \to s\gamma$ process in the SUSY SU(5) GUT with N_R model and the LRSM. The ratio $|C_7'/C_7|$, the polarization parameter of photon, and the direct CP asymmetry in the process have been evaluated in both models. The time-dependent CP asymmetry seems to be the best way to find the NP effect. However, the combination of CP violation and photon polarization can discriminate NP beyond the SM at the end. Furthermore, there might be a region where the determination of photon polarization is more sensitive for the new physics search than that of CP asymmetry.

Acknowledgments

We would like to thank to Y. Okada for fruitful discussion. This work is partially supported by Scientific Grant by Ministry of Education and Science, No. 24540272 and Grant-in-Aid for Scientific Research on Innovative Areas titled "Unification and Development of the Neutrino Science Frontier", No. 25105001. The work of R.T. are supported by Research Fellowships of the Japan Society for the Promotion of Science for Young Scientists.

6 Loop functions

We give loop functions [18] which are utilized in our analyses:

$$h_7(x) = -\frac{5x^2-3x}{12(1-x)^2} - \frac{3x^2-2x}{6(1-x)^3}\log x, \tag{6.1}$$

$$h_8(x) = -\frac{x^2-3x}{4(1-x)^2} + \frac{x}{2(1-x)^3}\log x, \tag{6.2}$$

$$f_{7,8}^{(1)}(x,y) = \frac{2}{x-y}(f_{7,8}^{(2)}(x) - f_{7,8}^{(2)}(y)), \tag{6.3}$$

$$f_7^{(2)}(x) = -\frac{13-7x}{24(1-x)^3} - \frac{3+2x-2x^2}{12(1-x)^4}\log x, \tag{6.4}$$

JHEP03(2015)160

$$f_8^{(2)}(x) = \frac{1+5x}{8(1-x)^3} + \frac{x(2+x)}{4(1-x)^4}\log x, \tag{6.5}$$

$$f_{\rm LR}(x) = -\frac{x^2+x+4}{4(1-x)^2} - \frac{3x}{2(1-x)^2}\log x, \tag{6.6}$$

$$g_7^{(1)}(x) = -\frac{2(1+5x)}{9(1-x)^3} - \frac{4x(1+x)}{3(1-x)^5}\log x, \tag{6.7}$$

$$g_8^{(1)}(x) = \frac{11+x}{3(1-x)^3} + \frac{9+16x-x^2}{6(1-x)^4}\log x, \tag{6.8}$$

$$g_7^{(2)}(x) = -\frac{2(1+10x+x^2)}{9(1-x)^4} - \frac{4x(1+x)}{3(1-x)^5}\log x, \tag{6.9}$$

$$g_8^{(2)}(x) = \frac{53+44x-x^2}{12(1-x)^4} + \frac{3+11x+2x^2}{2(1-x)^5}\log x, \tag{6.10}$$

$$D_0'(x) = \frac{-8x^3-5x^2+7x}{24(x-1)^3} + \frac{3x^3-2x^2}{4(x-1)^4}\log x, \tag{6.11}$$

$$A_{\rm LR}(x) = \frac{-5x^2+31x-20}{6(x-1)^2} - \frac{3x^2-2x}{(x-1)^3}\log x, \tag{6.12}$$

$$A_H^2(x) = \frac{22x^3-53x^2+25x}{72(x-1)^3} - \frac{3x^3-8x^2+4x}{12(x-1)}\log x. \tag{6.13}$$

7 Mass insertion parameters

The mass insertion parameters are defined as (e.g., see [36])

$$(\delta_q^{XX})_{ij} \equiv \frac{(m^2_{\tilde{q}_X})_{ij}}{\tilde{m}^2_{\tilde{f}}}, \tag{7.1}$$

$$(\delta_d^{XY})_{ij} \equiv \frac{v_d(A_d - \mu t_\beta)_{ij}}{\tilde{m}^2_{\tilde{f}}}, \tag{7.2}$$

$$(\delta_u^{XY})_{ij} \equiv \frac{v_u(A_u - \mu\cot)_{ij}}{\tilde{m}^2_{\tilde{f}}}, \tag{7.3}$$

with $X \neq Y$ where $\tilde{m}^2_{\tilde{f}}\,(\tilde{f} = \tilde{u}\,, \tilde{d})$ denotes up- and down-type averaged squark mass, and the numerator of eq. (7.1) can be written as

$$(m^2_{\tilde{u}_L})_{ij} \simeq -V_{3i}V^*_{3j}\frac{f_t^2}{(4\pi)^2}(3m_0^2 + A_0^2)\left(2\log\frac{M^2_{\rm pl}}{M^2_{H_c}} + \log\frac{M^2_{H_c}}{M^2_{\rm SUSY}}\right), \tag{7.4}$$

$$(m^2_{\tilde{u}_R})_{ij} \simeq -e^{-i\varphi_{u_{ij}}}V^*_{3i}V_{3j}\frac{2f_b^2}{(4\pi)^2}(3m_0^2 + A_0^2)\log\frac{M^2_{\rm pl}}{M^2_{H_c}}, \tag{7.5}$$

$$(m^2_{\tilde{d}_L})_{ij} \simeq -V^*_{i3}V_{j3}\frac{2f_t^2}{(4\pi)^2}(3m_0^2 + A_0^2)\left(3\log\frac{M^2_{\rm pl}}{M^2_{H_c}} + \log\frac{M^2_{H_c}}{M^2_{\rm SUSY}}\right), \tag{7.6}$$

$$(m^2_{\tilde{d}_R})_{ij} \simeq -e^{-i\varphi_{d_{ij}}}U^*_{ki}V_{kj}\frac{f^2_{\nu_k}}{(4\pi)^2}(3m_0^2 + A_0^2)\log\frac{M^2_{\rm pl}}{M^2_{H_c}}. \tag{7.7}$$

Here, m_0 and A_0 are the universal scalar mass and trilinear coupling, respectively.

JHEP03(2015)160

References

[1] R. Barbieri and L.J. Hall, *Signals for supersymmetric unification*, *Phys. Lett.* **B 338** (1994) 212 [hep-ph/9408406] [INSPIRE].

[2] R. Barbieri, L.J. Hall and A. Strumia, *Violations of lepton flavor and CP in supersymmetric unified theories*, *Nucl. Phys.* **B 445** (1995) 219 [hep-ph/9501334] [INSPIRE].

[3] Y. Kuno and Y. Okada, *Proposed $\mu \to e\gamma$ search with polarized muons*, *Phys. Rev. Lett.* **77** (1996) 434 [hep-ph/9604296] [INSPIRE].

[4] M. Gronau, Y. Grossman, D. Pirjol and A. Ryd, *Measuring the photon polarization in $B \to K\pi\pi\gamma$*, *Phys. Rev. Lett.* **88** (2002) 051802 [hep-ph/0107254] [INSPIRE].

[5] M. Gronau and D. Pirjol, *Photon polarization in radiative B decays*, *Phys. Rev.* **D 66** (2002) 054008 [hep-ph/0205065] [INSPIRE].

[6] B. Grinstein, Y. Grossman, Z. Ligeti and D. Pirjol, *The photon polarization in $B \to X\gamma$ in the standard model*, *Phys. Rev.* **D 71** (2005) 011504 [hep-ph/0412019] [INSPIRE].

[7] Y.Y. Keum, M. Matsumori and A.I. Sanda, *CP asymmetry, branching ratios and isospin breaking effects of $B \to K^*\gamma$ with perturbative QCD approach*, *Phys. Rev.* **D 72** (2005) 014013 [hep-ph/0406055] [INSPIRE].

[8] LHCb collaboration, *Observation of photon polarization in the $b \to s\gamma$ transition*, *Phys. Rev. Lett.* **112** (2014) 161801 [arXiv:1402.6852] [INSPIRE].

[9] D. Melikhov, N. Nikitin and S. Simula, *Probing right-handed currents in $B \to K^*\ell^+\ell^-$ transitions*, *Phys. Lett.* **B 442** (1998) 381 [hep-ph/9807464] [INSPIRE].

[10] C.S. Kim, Y.G. Kim, C.-D. Lu and T. Morozumi, *Azimuthal angle distribution in $BK^*(\to Kpi)\ell^+\ell^-$ at low invariant $m_{\ell^+\ell^-}$ region*, *Phys. Rev.* **D 62** (2000) 034013 [hep-ph/0001151] [INSPIRE].

[11] D. Becirevic, E. Kou, A. Le Yaouanc and A. Tayduganov, *Future prospects for the determination of the Wilson coefficient $C'_{7\gamma}$*, *JHEP* **08** (2012) 090 [arXiv:1206.1502] [INSPIRE].

[12] J.M. Soares, *CP violation in radiative b decays*, *Nucl. Phys.* **B 367** (1991) 575 [INSPIRE].

[13] M. Endo and N. Yokozaki, *Large CP-violation in B_s Meson Mixing with EDM constraint in Supersymmetry*, *JHEP* **03** (2011) 130 [arXiv:1012.5501] [INSPIRE].

[14] A.J. Buras, *Weak Hamiltonian, CP-violation and rare decays*, hep-ph/9806471 [INSPIRE].

[15] A.L. Kagan and M. Neubert, *QCD anatomy of $B \to X_{s\gamma}$ decays*, *Eur. Phys. J.* **C 7** (1999) 5 [hep-ph/9805303] [INSPIRE].

[16] M. Ciuchini, E. Franco, G. Martinelli, L. Reina and L. Silvestrini, *Scheme independence of the effective Hamiltonian for $b \to s\gamma$ and $b \to sg$ decays*, *Phys. Lett.* **B 316** (1993) 127 [hep-ph/9307364] [INSPIRE].

[17] A.J. Buras, M. Misiak, M. Münz and S. Pokorski, *Theoretical uncertainties and phenomenological aspects of $B \to X_{s\gamma}$ decay*, *Nucl. Phys.* **B 424** (1994) 374 [hep-ph/9311345] [INSPIRE].

JHEP03(2015)160

[18] W. Altmannshofer, A.J. Buras, S. Gori, P. Paradisi and D.M. Straub, *Anatomy and Phenomenology of FCNC and CPV Effects in SUSY Theories*, *Nucl. Phys.* **B 830** (2010) 17 [arXiv:0909.1333] [INSPIRE].

[19] Particle Data Group collaboration, K.A. Olive et al., *Review of particle physics*, *Chin. Phys.* **C 38** (2014) 090001.

[20] M.C. Gonzalez-Garcia, M. Maltoni and T. Schwetz, *Updated fit to three neutrino mixing: status of leptonic CP-violation*, *JHEP* **11** (2014) 052 [arXiv:1409.5439] [INSPIRE].

[21] E. Kou, A. Le Yaouanc and A. Tayduganov, *Determining the photon polarization of the $b \to s\gamma$ using the $B \to K_1(1270)\gamma \to (K\pi\pi)\gamma$ decay*, *Phys. Rev.* **D 83** (2011) 094007 [arXiv:1011.6593] [INSPIRE].

[22] J.C. Pati and A. Salam, *Lepton Number as the Fourth Color*, *Phys. Rev.* **D 10** (1974) 275 [*Erratum ibid.* **D 11** (1975) 703-703] [INSPIRE].

[23] R.N. Mohapatra and J.C. Pati, *Left-Right Gauge Symmetry and an Isoconjugate Model of CP-violation*, *Phys. Rev.* **D 11** (1975) 566 [INSPIRE].

[24] R.N. Mohapatra and J.C. Pati, *A Natural Left-Right Symmetry*, *Phys. Rev.* **D 11** (1975) 2558 [INSPIRE].

[25] G. Senjanović and R.N. Mohapatra, *Exact Left-Right Symmetry and Spontaneous Violation of Parity*, *Phys. Rev.* **D 12** (1975) 1502 [INSPIRE].

[26] U. Amaldi et al., *A Comprehensive Analysis of Data Pertaining to the Weak Neutral Current and the Intermediate Vector Boson Masses*, *Phys. Rev.* **D 36** (1987) 1385 [INSPIRE].

[27] M. Blanke, A.J. Buras, K. Gemmler and T. Heidsieck, *$\Delta F = 2$ observables and $B \to X_q\gamma$ decays in the left-right model: Higgs particles striking back*, *JHEP* **03** (2012) 024 [arXiv:1111.5014] [INSPIRE].

[28] E. Kou, C.-D. Lü and F.-S. Yu, *Photon Polarization in the $b \to s\gamma$ processes in the Left-Right Symmetric Model*, *JHEP* **12** (2013) 102 [arXiv:1305.3173] [INSPIRE].

[29] Y. Zhang, H. An, X. Ji and R.N. Mohapatra, *General CP-violation in Minimal Left-Right Symmetric Model and Constraints on the Right-Handed Scale*, *Nucl. Phys.* **B 802** (2008) 247 [arXiv:0712.4218] [INSPIRE].

[30] G. Senjanović, *Spontaneous Breakdown of Parity in a Class of Gauge Theories*, *Nucl. Phys.* **B 153** (1979) 334 [INSPIRE].

[31] M.A.B. Beg, R.V. Budny, R.N. Mohapatra and A. Sirlin, *Manifest Left-Right Symmetry and Its Experimental Consequences*, *Phys. Rev. Lett.* **38** (1977) 1252 [*Erratum ibid.* **39** (1977) 54] [INSPIRE].

[32] T. Hurth, E. Lunghi and W. Porod, *Untagged $\bar{B} \to X_{s+d}\gamma$ CP asymmetry as a probe for new physics*, *Nucl. Phys.* **B 704** (2005) 56 [hep-ph/0312260] [INSPIRE].

[33] Quark Flavor Physics Working Group collaboration, J.N. Butler et al., *Working Group Report: Quark Flavor Physics*, arXiv:1311.1076 [INSPIRE].

[34] R.-H. Li, C.-D. Lu and W. Wang, *Branching ratios, forward-backward asymmetries and angular distributions of $B \to K_2^* l^+ l^-$ in the standard model and new physics scenarios*, *Phys. Rev.* **D 83** (2011) 034034 [arXiv:1012.2129] [INSPIRE].

[35] S. Jäger and J. Martin Camalich, *On $B \to V\ell\ell$ at small dilepton invariant mass, power corrections and new physics*, *JHEP* **05** (2013) 043 [arXiv:1212.2263] [INSPIRE].

[36] J. Hisano, M. Kakizaki, M. Nagai and Y. Shimizu, *Hadronic EDMs in SUSY* SU(5) *GUTs with right-handed neutrinos*, *Phys. Lett.* **B 604** (2004) 216 [hep-ph/0407169] [INSPIRE].

JHEP03(2015)160